Observation of near-surface damage by phonon scattering

R. Maboudian,* C. Carraro,† D. L. Goodstein, R. M. Housley, and T. A. Tombrello
Department of Condensed Matter Physics, California Institute of Technology, 114-36, Pasadena, California 91125
(Received 23 May 1988)

We have investigated the feasibility of phonon-reflection techniques as nondestructive means to probe surface and/or near-surface damage in otherwise highly perfect crystals. An UHV liquid-helium stage, suitable for phonon-reflection measurements, was installed on a beam line of a tandem van de Graaff accelerator which was used to implant MeV ions into the substrate in order to modify the surface region *in situ*. Here, we report our investigation on the effects of 1-MeV Ar^+ implantation in Al_2O_3 single crystals by monitoring the reflection of terahertz (THz) phonons (50-Å wavelength) from the implanted region. The results are compared to other surface techniques. Using a 15-kV ion gun on the same beam line, we have also bombarded Al_2O_3 crystals coated with thin films of gold. The effects of a 7.5-keV Ar^+ beam on this Au-Al_2O_3 system are also discussed in this paper.

I. INTRODUCTION

For some years, we have investigated problems such as the anomalous low-temperature transmission of heat across various interfaces[1–4] (a problem called the Kapitza anomaly) and also the desorption mechanism of He thin films,[5–7] using ballistic phonons generated by heat pulses.[8] A schematic diagram of the experiment relevant to this paper is depicted in Figs. 1(a) and 1(b). A thin metallic film (in our case 500-Å Nichrome) is evaporated on one side of a sapphire (Al_2O_3) single crystal. By Joule heating, thermal phonons are radiated into the substrate. If the crystal has very few impurities (i.e., low phonon-defect scattering) and is at a temperature sufficiently low with respect to the Debye temperature of the solid (i.e., negligible dispersion effects as well as low phonon-phonon interaction), the phonons travel macroscopic distances without being scattered. Sapphire easily satisfies these criteria due to its very high Debye temperature[9] ($\sim$1000 K), low isotopic impurity (0.204% due to ^{18}O), and advanced methods of single-crystalline growth (low impurity concentration). Because of the latter, it is possible to get large crystals which enable us to neglect wall effects. The ejected phonons traverse the crystal, are reflected from the surface (usually under vacuum), and, after traversing the crystal again, are detected by means of a superconducting Sn bolometer (2000 Å thick). Using very short (30-nsec duration) heat pulses as well as small heaters and bolometers (0.1-mm^2 area), we achieve time resolution of the order of a few tens of nsec.[6] In this way one is able to resolve various phonon polarizations (one longitudinal, two transverse, and up to six mode converted) due to their different paths and group velocities, and thus their arrival times [Fig. 1(c)] at the detector.[1,2] Because of the nonideality of the surface, some of the phonons are reflected specularly and some diffusely (normally showing up as a long tail superimposed on the specular peaks). Taking advantage of the crystalline anisotropy of sapphire, it has been shown that one can find relative positions for heater and bolometer for which diffusely scattered phonons are preferentially focused in the direction of the bolometer and detected as a separate broad peak in a plot of signal versus time.[2] A typical signal in this orientation is shown in Fig. 2. If one introduces liquid helium (LHe) or even a few monolayers of He adsorbed to the outside of the reflecting surface, the diffuse peak is dramatically reduced while the specular peaks remain the same.[2] Briefly, this arises in the following way.[3] Considering the transmission probability (α) of phonons across any *ideal* solid-LHe interface using classical continuum mechanics, the considerably smaller speed of sound, as well as the smaller mass density of LHe compared to any other solid, would yield $\alpha \sim 0.01$ due to a large acoustic impedance mismatch. However, experimentally one observes α's of about 0.5. Based on our experiments as well as other similar experiments, it was realized that there are two transmission components. One, as expected, obeys the acoustic mismatch model (the specular peaks in our experiment). The other is anomalous (the diffuse signal, which disappears when in contact with LHe). It has been demonstrated experimentally[10,11] that the anomalous component is a consequence of surface defects which, once removed, leave only the expected acoustic-mismatch result and no anomaly. Originally it was though that this happened only for a solid-LHe interface, but later it was shown that similar process occurs for other systems[12] (e.g., sapphire–solid-Ar) as well. Several models have been proposed,[13,14] but the exact microscopic nature of this process remains unresolved, mainly due to the as yet poor understanding of the exact mechanism of the diffuse scattering at nonideal surfaces.

It has been shown[15–17] that the low-temperature thermal conductivity measurements in the boundary scattering regime are also sensitive to the nature of phonon reflection (diffuse versus specular) at surfaces and interfaces. Pohl and Stritzker[15] have reported such measurements on sapphire samples with a variety of surface treatments including ion bombardment in an attempt to study the causes of diffuse phonon scattering at crystal surfaces.

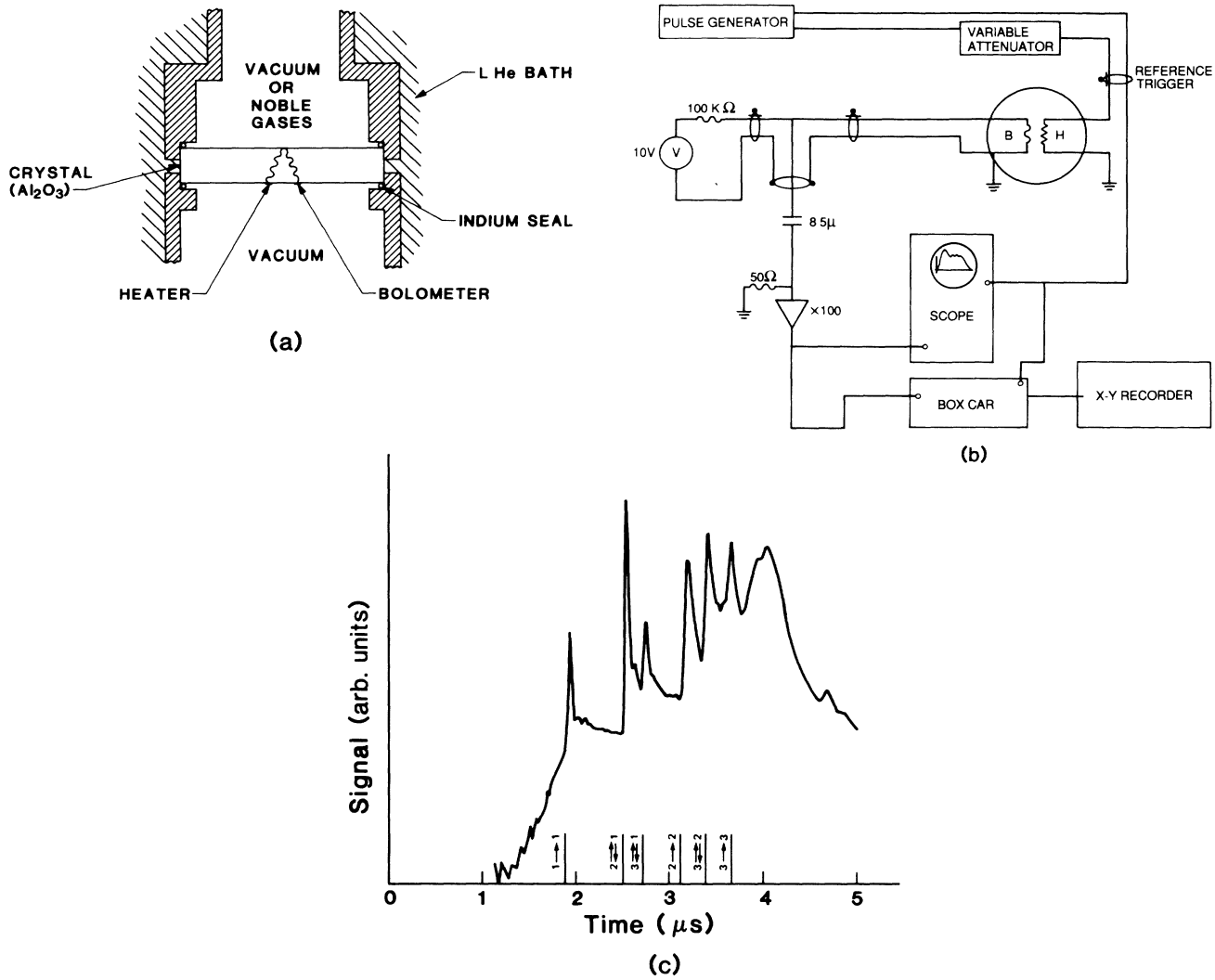

FIG. 1. (a) Schematic diagram of the geometry of a ballistic-phonon-reflection experiment. A thin-film heater is evaporated on one side of an Al_2O_3 single crystal. By pulsing the heater, phonons are radiated into the substrate. They traverse the crystal, reflect from the other surface, and are detected using a Sn superconducting bolometer. (b) Schematic diagram of the electronics used in phonon reflection experiment. A pulse generator with fast rise and fall times (~ 5 nsec) is used to pulse the heater and raise its temperature from 3.7 K (ambient temperature) to ~ 19 K. Typical values for the pulse duration is 30 nsec and for the pulse repetition rate is 100 kHz. Some distance away from the heater is a superconducting bolometer which is biased in the middle of its superconducting transition. Reflected phonons, arriving at the bolometer, raise its temperature, leading in turn to a change in its resistance and thus a change in the voltage across the device. Then, using a preamplifier, this change is amplified 100 times and after being averaged by a boxcar integrator, is recorded on an X-Y recorder. (c) Reflection signal showing various reflection processes (taken from Ref. 2). Polarizations are labeled 1,2,3 in order of wave speed (1 is longitudinal, 2 is fast transverse, and 3 is slow transverse), arrows indicating the change in polarization upon reflection. Heater and bolometer are separated by 9 mm along the X axis (twofold symmetry axis).

Due to the extreme sensitivity of our phonon-focused diffuse-peak technique, we decided to carry out a similar investigation. However, we wanted to have the capability to alter the surface region in a controlled way and under UHV conditions and to study simultaneously the scattering of phonons from such modifications. Ion beams are particularly suitable for this purpose because one is able to vary the depth at which the damage is introduced by varying their energy and also change the extent of the damage by changing the dose.

The general plan of attack is as follows. The introduction of new defects by the ion beam should enhance the diffuse signal in Fig. 2 at the expense of the specular peaks. This result is expected when the beam sputters the surface, and also when a higher energy beam creates damage a few thousand angstroms inside the surface. If the enhanced diffuse scattering is close to the surface, it should then be possible to remove the diffuse bump by coating the surface with an adsorbed Ar film. If the damage is deep inside, the Ar film should have no effect.

As we shall see below, although a few mysteries do emerge from the results, these expectations are generally

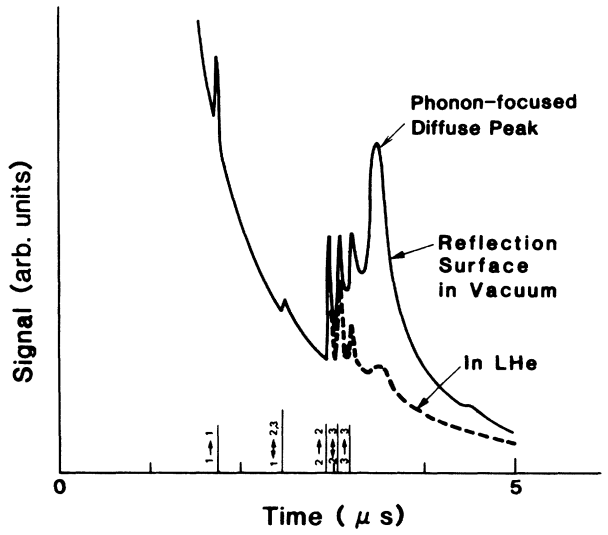

FIG. 2. Reflection signal for heater and bolometer displaced by 2 mm along the X axis (taken from Ref. 2). The solid curve is the signal with the reflection surface under vacuum. The sharp peaks are the specularly reflected phonons [labeled using the same notation as in Fig. 1(c)] whereas the broad peak is from the diffusely scattered phonons which, due to anisotropy of Al_2O_3, are preferentially focused in the direction of the bolometer. The small peak at 4.5 μs is attributed to a double-reflection process. The dashed curve shows the effect of adding liquid He. The specular peaks remain essentially unchanged whereas the diffuse signal is dramatically suppressed (Kapitza anomaly). The long decaying background, onto which the reflection signal is superimposed, is thought to be due to bulk scattering.

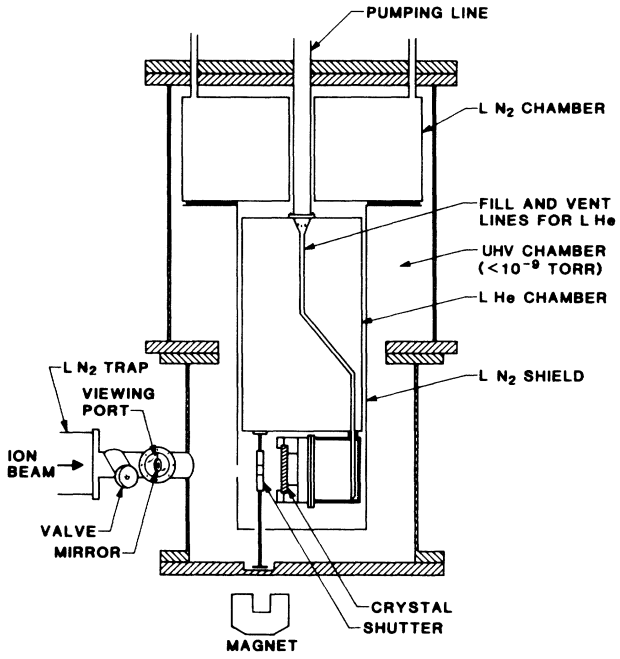

FIG. 3. Schematic diagram of the UHV cryostat. The crystal, looking into the beam line, is mounted on a copper block which is in direct contact with the LHe bath. To reduce the heat loss due to room temperature radiation, the LHe reservoir is surrounded by a liquid-nitrogen (LN_2) chamber as well as a LN_2 radiation shield. The operating period is about 4 h and the lowest achievable temperature is ~ 2 K. To check the quality of the beam (its alignment, uniformity, etc.) a shutter is suspended from the LHe pot. When closed, the beam sees a quartz crystal, mounted on the shutter, which fluoresces due to the impinging ions. When the beam is in a satisfactory position, the shutter is open and the beam hits the crystal.

satisfied. Our conclusions are also supported by x-ray rocking curve measurements,[18] and by Monte Carlo simulations of the damage[19] done by the ion beams.

The paper is organized as follows. In Sec. II, we describe the experimental setup. In Sec. III we present our data for 1-MeV Ar^+ (in Sec. III A) and 7.5-keV Ar^+ irradiation (in Sec. III B). Finally, in Sec. IV we summarize the results, compare our results to those of Pohl and Stritzker,[15] and end with some concluding remarks.

II. EXPERIMENTS

A schematic diagram of the experimental setup is shown in Fig. 3. It is a UHV (10^{-9} Torr or better) homemade cryostat. The crystal is mounted on a copper block at the bottom of the LHe reservoir. Its surface is then placed in the beam line of a tandem van de Graaff accelerator, also equipped with a keV sputtering setup as shown in Fig. 4. A liquid-nitrogen in-line trap enables us to maintain a pressure difference better than 2 orders of magnitude between the beam line (10^{-7} Torr) and the cryostat. In order to be able to position the beam with respect to the crystal, a magnetically operated shutter is placed in front of the crystal (suspended from the LHe reservoir). In its normal position (without any magnetic field), a quartz disk (1 cm in diameter) covered with a thin Au film intercepts the beam. The beam causes the quartz to fluoresce, and using the mirror shown in the

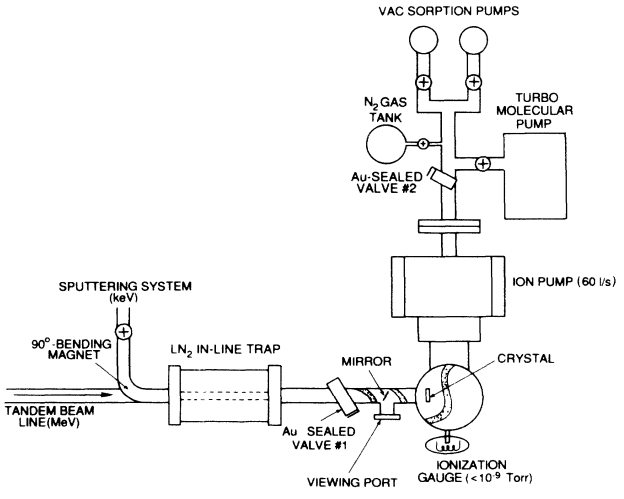

FIG. 4. Top view of the experimental setup, showing the pumping system as well as the beam line. The MeV implantation beam was generated by a tandem van de Graaff accelerator. Using a 15-kV ion gun, a low-energy (7.5 keV) sputtering beam was produced and bent into the main beam line via a 90° bending magnet. Using a mirror angle with a viewing port, one can see the beam spot on the shutter right before it hits the crystal.

Fig. 4 we can check the beam spot (its alignment, uniformity, etc.). Then by applying a magnetic field from outside we can open the shutter and introduce the beam to the crystal. The crystal is 5.7 cm in diameter and 1 cm thick and the maximum beam spot is 6 mm in diameter hitting the center of the crystal.

In the previous work presented in Refs. 1 and 2, the sapphire crystals were grown by Union Carbide Corporation using Czochralski's method and the surfaces were mechanically polished. In the present investigation, in order to have a better surface polish, the crystal, grown by Union Carbide Corporation, was chemi-mechanically polished by Crystal System Inc.[20] Electron channeling pattern has been observed from this crystal indicating its high quality polish. Also the phonon reflection signal from this crystal has a noticeably smaller diffuse component than observed in the previous investigation (Refs. 1 and 2), pointing to the superior surface of this crystal.

We wanted to see what happens to both specular and diffuse reflections as a consequence of ion bombardment. But since the main contribution to the diffuse peak[2] is due to reflection from a different spot on the surface than the specular peaks (7 to 8 mm away in our geometry—too far for the beam spot to cover), we had to use two different sets of devices [Fig. 5(a)], one at the center of the crystal (H_0-B_0), such that the beam would influence the specular peaks and one displaced from the center (H_1-B_1) such that the diffuse contribution to the signal would come from the central region. Thus we were monitoring the same beam spot using two sets of devices. This turned out to be an advantage, as we shall see below, since in each case the part of the signal that changed could be normalized by the part that did not.

For the experiments reported in this article, the reflection surface has been covered with 750 Å of Au as shown in Fig. 5(b). This way, we could use the gold as a means to measure the beam dose on the sample by current integration. Also, in the case of the keV beam there was no easy way of neutralizing the bombarded crystal and thus without the Au there could have been serious charging problems. Before we state the results, it is worth noting that we took as much care as possible in cleaning the crystal and also evaporating the Au film. We etched Al_2O_3 in hot (220° C) phosphoric acid[21] and then immediately placed it in a UHV bell jar. The base pressure was 10^{-9} Torr and it increased to 10^{-8} Torr during the evaporation. Figure 6 shows the phonon signal with and without the Au film. Even though the specular peaks essentially remain the same, contrary to expectation the diffuse peak is almost completely gone when

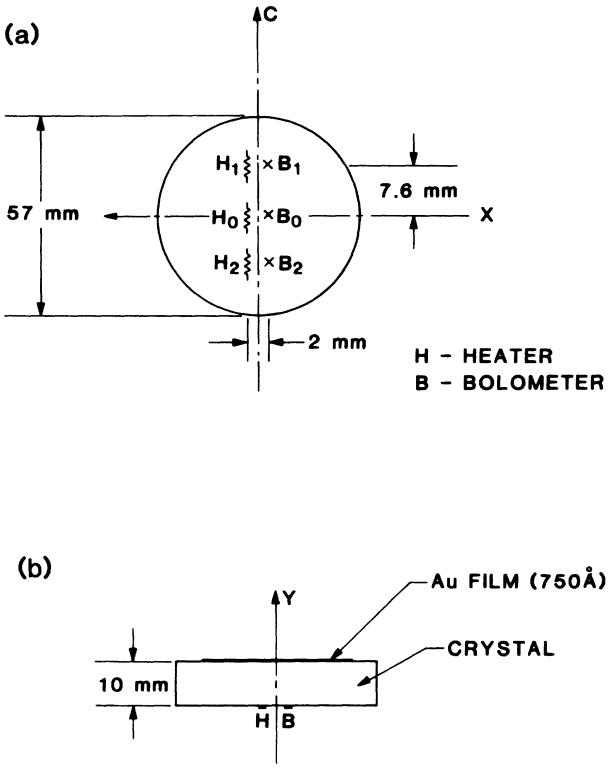

FIG. 5. (a) Top view of the crystal showing the positions of the heaters and bolometers used in the experiments reported here. The beam (~6 mm in diameter) hits the center of the crystal. In this case, the specular peaks of the H_0-B_0 set are affected as well as the diffuse peak of the H_1-B_1 set. Neither the specular peaks nor the diffuse peak of the H_2-B_2 set should see the incident beam and thus we use this set to make sure nothing spurious is happening. (b) Side view of the crystal showing the gold film overlaid on the crystal. Sapphire, being an insulator, cannot be directly used to measure the beam current and thus the beam dose. To be able to do so, a 750-Å Au film was overlaid on the surface. Also in the case of the low-energy (keV) beam, the gold film is essential; without it the crystal would charge up and repel the beam.

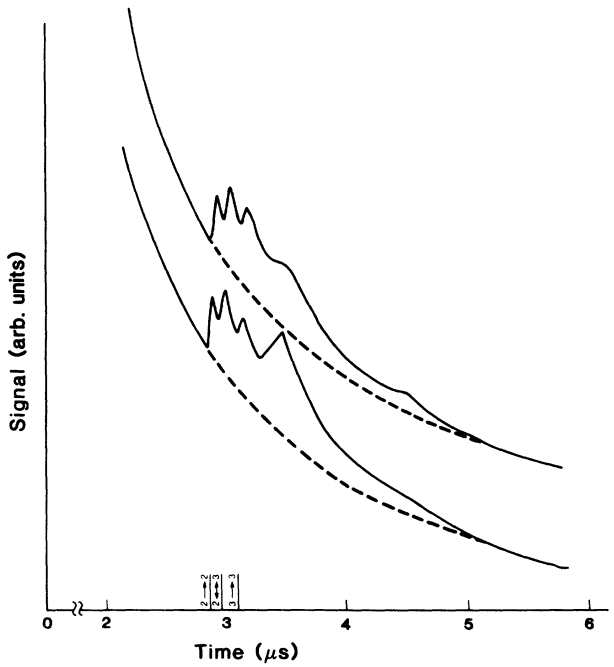

FIG. 6. Phonon-reflection signal for the same geometry as in Fig. 2. The lower curve is for the reflection surface in vacuum and the upper curve is with 750 Å of Au evaporated onto the surface. Though the specular peaks remain essentially unchanged, the diffuse peak is considerably suppressed.

Au is present, a result resembling the effect of He and other noble-gas films. This observation is quite surprising in view of the fact that the gold film adheres very poorly to the substrate.[22] In practice, this behavior turned out to be quite useful because by initially suppressing the diffuse signal, we could monitor how it would change under the various modifications.

III. RESULTS

A. 1-MeV Ar^+ beam implanation

Figure 7(b) shows the effect of 1-MeV Ar^+ implantation on the specular peaks (H_0-B_0 signal) and Fig. 7(a) shows that on the diffuse contribution (H_1-B_1 signal). The basic features are reduction of specular reflection and enhancement of diffuse scattering. To quantify this result somewhat, we needed better estimates for the sizes of the various peaks. For this, we needed to subtract the large background on which the reflection peaks are superimposed. The source of this background has been attributed to bulk scattering.[23] By fitting a cubic spline to the two ends of this background where it is expected to be free of the influence of the reflection signal and interpolating the curve in between, we were able to subtract this background as shown in Fig. 8(a). The next step was to deconvolve the various reflection peaks, which proved to be a much harder task. The detected widths of the peaks are consequences of several processes: some diffuse scattering from the surface falling into the solid angle subtended by the bolometer, bulk scattering, electronics, etc., making it difficult to deconvolve these peaks reliably. Instead, we made the assumption that all the specular peaks have the same line shape and used the longitudinal peak, which is unaffected by other peaks, as a model. This permitted us to deconvolve the three overlapping specular peaks (two transverse and one mode converted), thus segregating out the diffuse contribution. From this, one can see [Fig. 8(b)] that basically the height of the fast transverse (FT) mode and the diffuse peak are unaffected by the other peaks (after background subtraction). Thus, we took either the height of the FT mode or that of the diffuse contribution as a fixed standard in various modifications.

Adopting this technique, in Fig. 9(a) we have plotted the height of the FT mode (normalized to the height of the unaffected diffuse peak) as a function of the dose for the H_0-B_0 signal. Similarly in Fig. 9(b), the height of the diffuse peak (normalized to the unaffected FT peak) is plotted for the H_1-B_1 signal. The basic trend is that by implantation the diffuse contribution increases and the specular signals are suppressed (though more abruptly). The effect saturates by a dose of about 8×10^{13} atoms/cm^2 for the specular peak and at a dose of 6×10^{14} ions/cm^2 for the diffuse peak.

To estimate the ion-beam range and the extent of the damage, we used the TRIM (Transport of Ions in Matter—version '87) Monte Carlo simulation.[19] The method consists of following a large number of individual ions or particles in an amorphous target (with atoms at random positions). Each step begins with a given energy, position, and direction. The particle is assumed to

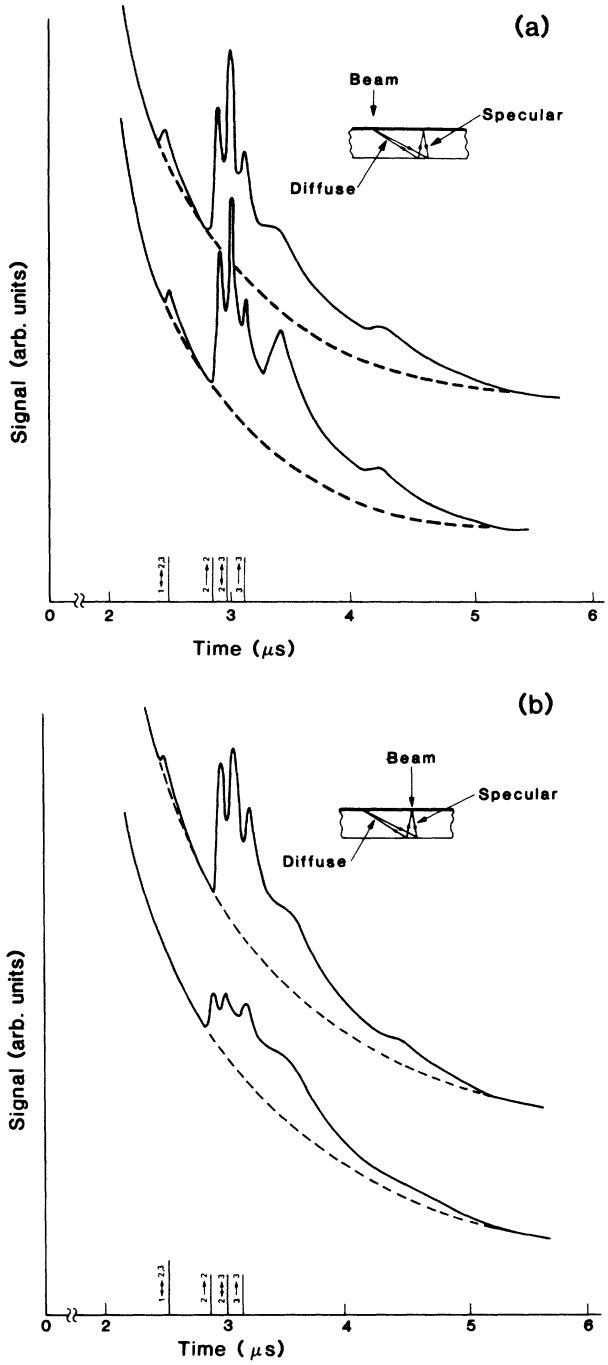

FIG. 7. (a) Phonon-reflection signal showing the effect of 1-MeV Ar^+ implantation on the diffuse peak as shown in the inset. The reflection surface is covered with 750 Å of Au. The upper curve is the signal from a virgin crystal whereas in the lower trace, 1-MeV Ar^+ is implanted in the substrate ($\sim7.3\times10^{14}$ Ar^+/cm^2). The inset shows that in this case, the beam is only affecting the diffuse peak as can be seen from the traces. The dashed curves are the spline fits to the background (see the text). (b) Reflection signals showing the effect of 1-MeV Ar^+ implantation on the specular peaks as shown in the inset. The upper trace is the signal prior to implantation and the curve is taken after the 2.4×10^{14} Ar^+/cm^2 implantation dose. As seen in the inset, in this case, the beam is affecting the specular peaks only. The dashed curves are the spline fits to the background (see the text).

change direction as a result of binary nuclear collisions and move in straight paths between each collision. The energy is reduced as a result of electronic (inelastic) and nuclear energy losses. These two processes are assumed to be independent and thus particles lose energy in discrete amounts in nuclear collisions and lose energy continuously from electron interactions. The energy transferred to a target is analyzed further to obtain information such as damage energy and number of atom displacements produced in a collision cascade.

Figure 10 shows a TRIM simulation for a 1-MeV Ar^+ beam on Al_2-O_3. It shows [Fig. 10(a)] that the ions penetrate into the target with a mean range of 5500 Å and straggling of 1000 Å. The calculation also indicates that target-atom displacement has occurred even at the surface. [Fig. 10(b)] possibly leading to some sputtering.[24] To find out whether the change in the phonon signal is due to the modifications occurring at the surface or deeper inside, thermal neutral Ar atoms were introduced to the surface creating an adsorbed film. If the appearance of the diffuse scattering is strictly a surface phenomenon, we expected it to disappear as observed in previous experiments.[12] Instead, we saw no change in the diffuse contribution leading us to believe that phonons were responding to the modification inside the material and thus, we have shown here that the diffuse scattering is not necessarily associated with the surface. After taking the crystal out of the chamber, we carried out Ruth-

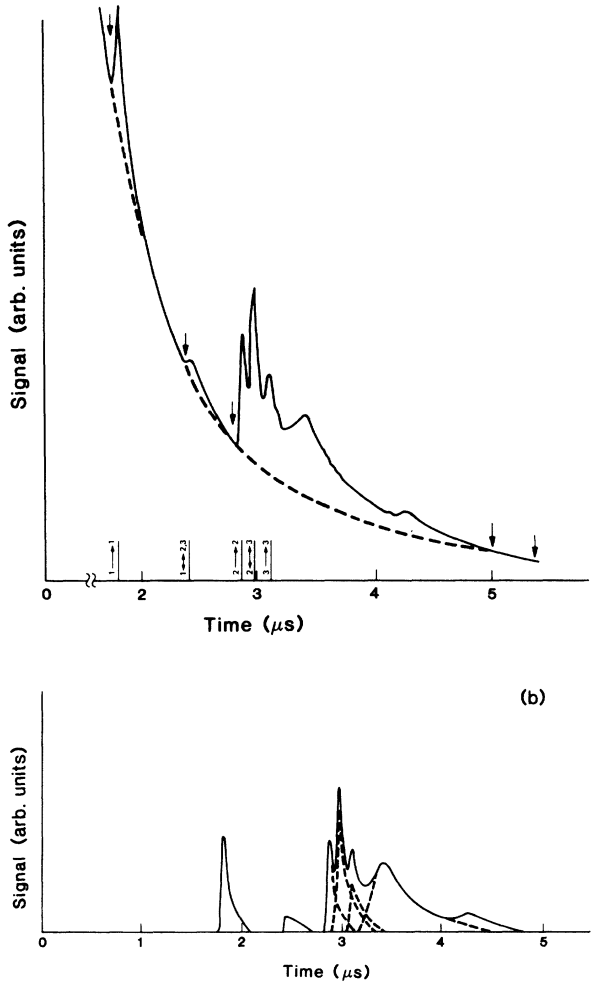

FIG. 8. (a) Reflection signal showing the background subtraction scheme. Arrows indicate the points where, we believe, the background is free from the influence of the reflection peaks. To these points (normally six), a cubic spline is fitted (dashed curve). (b) The reflection signal with the background subtracted (a) showing the deconvolution scheme. By assuming the line shapes of the two transverse peaks ($2\rightarrow2, 3\rightarrow3$) and the mode-converted peak ($2\leftrightarrow3$) to be the same as that of the longitudinal peak ($1\rightarrow1$), one can successively deconvolve these three peaks and the diffuse peak. Note that the heights of the fast transverse mode ($2\rightarrow2$) and the diffuse peak are unaffected by the other peaks and therefore we have used two peaks as means to quantify the effect of each treatment.

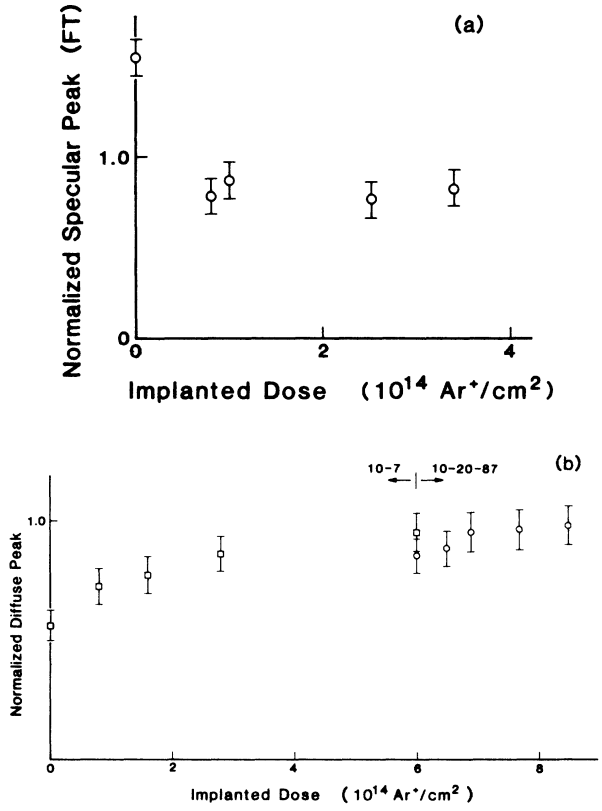

FIG. 9. (a) The height of the fast transverse peak, normalized to the amplitude of the unaffected diffuse peak, as a function of the 1-MeV Ar^+ implanted dose. The signal is saturated by the dose of 8×10^{13} Ar/cm^{-2}. (b) The height of the diffuse signal, normalized to the amplitude of the unaffected fast transverse peak, as a function of the implanted 1-MeV Ar^+ dose. Here the signal is saturated by a dose of 6×10^{14} ions/cm^2. The error bars are due to uncertainty in the reproducibility of the biasing point of the bolometer after each measurement in addition to the reading error. The squares (□) are the data taken on October 7, 1987 whereas the circles (○) are taken on October 20, 1987. In between, the cryostat was warmed up to room temperature and cooled back down. We see some weak evidence for annealing of the induced damage.

erford backscattering on the 1-MeV Ar^+ implanted spot and we did not observe any change in the thickness of the gold with respect to the untreated substrate. This observation confirmed that the enhancement of the diffuse reflection was due to the damage deep inside the crystal, rather than being the result of the sputtering of the gold film.

To obtain a measure of the ion-beam damage, after taking the crystal out of the chamber we investigated the damaged region using the x-ray rocking technique. The basic principle behind this technique is the following.[25] The diffracted x-ray intensity profiles (rocking curves) are highly sensitive to depth-dependent strain and damage distributions as well as their lateral variation. If the lattice is strained say, in the direction perpendicular to the sample surface, this leads to a shift in the Bragg peak given by

$$\Delta\theta \rightarrow \Delta\theta - \epsilon^{\perp}\tan\theta_B \ , \tag{1}$$

where

$$\Delta\theta \equiv \theta - \theta_B \ ,$$

θ_B is the Bragg angle, and $\epsilon^{\perp}$ is the perpendicular strain.

In ion-implanted crystals, a significant fraction of atoms may be displaced from their lattice sites giving rise to a change in structure factor. If one assumes that the statistical distribution of displacements of atoms from their lattice positions has a Gaussian form, this leads to a mean structure factor given by

$$\langle F_H \rangle = e^{-W} F_H^0 \ , \tag{2}$$

where F_H^0 is the structure factor of the undamaged crystal for planes signified by the H Miller indices, and

$$W = -\frac{8\pi^2}{\lambda^2}(\sin^2\theta_B)U^2 \ , \tag{3}$$

where U is the standard deviation of displacements and λ is the wavelength of the x ray. Then to find out the strain and damage distribution giving rise to the observed x-ray rocking curve, the affected region is represented by a set of diffracting laminae oriented parallel to the surface. A uniform strain $\epsilon^{\perp}$ and a random displacement standard deviation U are assigned to each layer. If the reflection power is less than 6% one can ignore extinction (i.e., multiple scattering) and use the kinematical x-ray model to determine the diffracted intensity profile by summing wave fields from the layers (taking account of phase and normal absorption). By trial and error, a strain and damage distribution is found for which the calculated rocking curve fits the measurements closely. However, the depth profiles of damage and strain found this way are not necessarily unique and one would need to have, by other means, some independent information about effect of the beam on the sample.

Figure 11 shows the normalized intensity of the

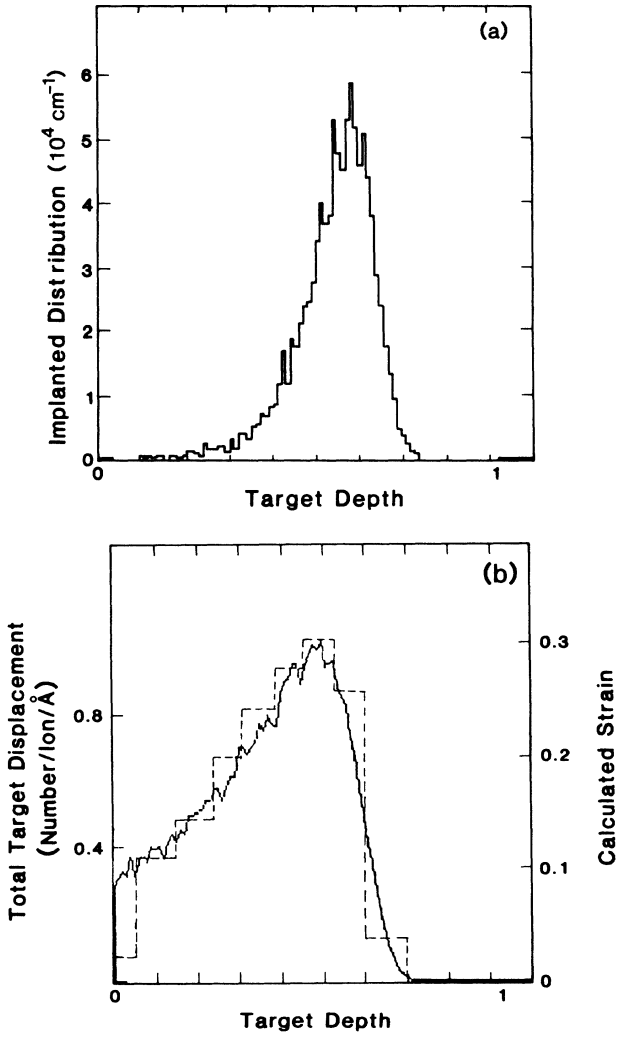

FIG. 10. (a) TRIM Monte Carlo simulation of the range of a 1-MeV Ar^+ beam in Al_2O_3. The mean range is about 5400 Å with a straggling of 900 Å. (b) The solid curve shows the TRIM results for target-atom displacement in the case of 1-MeV Ar^+ bombardment. The dashed curve is the strain distribution found by trial and error which led to a good fit to the x-ray rocking curve of Fig. 11 (see the text).

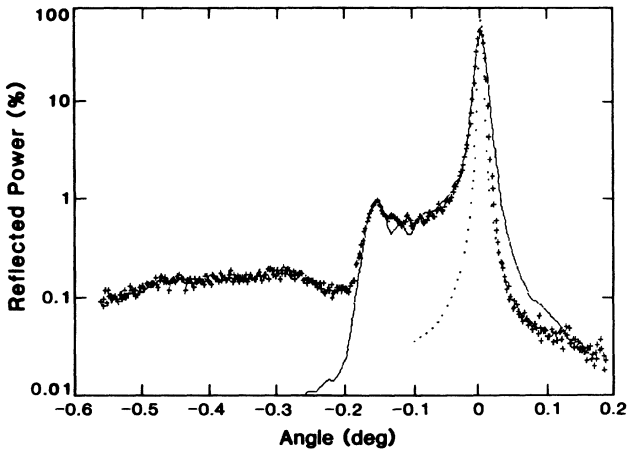

FIG. 11. X-ray rocking measurements on virgin as well as 1-MeV Ar^+ implanted Al_2O_3. The dots (·) are the measured intensity of the diffracted x ray for the virgin crystal as a function of the tilt angle about the substrate Bragg peak and the pluses (+) show the effect of the Ar^+ implantation. The solid curve is the calculated x-ray rocking intensity using kinematical x-ray model for the strain profile of Fig. 10(b).

diffracted beam on a virgin sample and also the implanted crystal. The diffracted peak is quite sharp and symmetric for the undamaged sample whereas in the case of the irradiated crystal, we see additional structure on the negative tail of the Bragg peak. By trial and error, we tried to reproduce the strain and damage profiles giving rise to the observed structure. We used the TRIM results as our initial guess. The dashed curve in Fig. 10(b) shows the strain distribution that reproduced the x-ray results relatively well for $\Delta\theta \lesssim -0.2°$. It is also very similar to the TRIM results. However, we are still puzzled by the long-decaying tail on the Bragg signal. Based on the kinematical x-ray model, Eq. (1), this tail corresponds to regions of higher strain than one deduces from the TRIM simulations assuming a linear relation between strain and displacement density. The x-ray rocking technique has been most extensively used to study radiation damage in semiconductors[26] and less so in insulators.[27] Due to this lack of information on insulators, the exact cause of this tail requires a more systematic investigation.

B. 7.5-keV Ar^+ beam

We have repeated the above procedure for keV Ar^+ beams. As mentioned earlier, to sputter Al_2O_3 we would have needed to keep the target from charging. Instead we chose to lay down a film of Au (750 Å) on the sapphire and see how bombarding the gold would alter the phonon-reflection signal. As before, the specular peaks remained essentially unaffected by the presence of the gold film (this was tested in another run by stripping the film away[22]), whereas the diffuse signal was dramatically suppressed.

The TRIM calculation shows that in the case of 7.5-keV Ar^+ beam, the beam penetrates into the sapphire substrate with a mean range of 50 Å and straggling of 30 Å. Thus, while removing gold, the beam is damaging the crystal to a depth of about 50 Å comparable to the wavelength of the phonons and thus altering the reflectivity of the surface.

The effect of 7.5 keV Ar^+ bombardment on the heat pulse signal is shown in Figs. 12(a) (phonon-focused diffuse peak) and 12(b) (specular peaks). Figure 13 shows the result of 7.5 keV Ar^+ sputtering of Au. The basic trend is similar to that of the MeV implantation: an abrupt decline in specular reflection [Fig. 13(a)] along with a more gradual increase in the diffuse component [Fig. 13(b)]. However, the effect is quantitatively different here in the sense that is seems to be more pronounced than in the case of the MeV implantation. The specular peaks are almost completely gone in contrast to a factor of 2 reduction in the deep implantation case. When considering the specular peaks, such a comparison is justified because as mentioned earlier, the gold film does not have any appreciable effect on the specular peaks. However, this is not the case for the diffuse signal. One must remember that the 7.5 keV beam removes the gold film as well as damaging the target and thus the enhancement of the diffuse peak is partly due to the damage introduced by the beam and partly due to the removal of the gold film. The cross ($\times$) in Fig. 13(b) shows

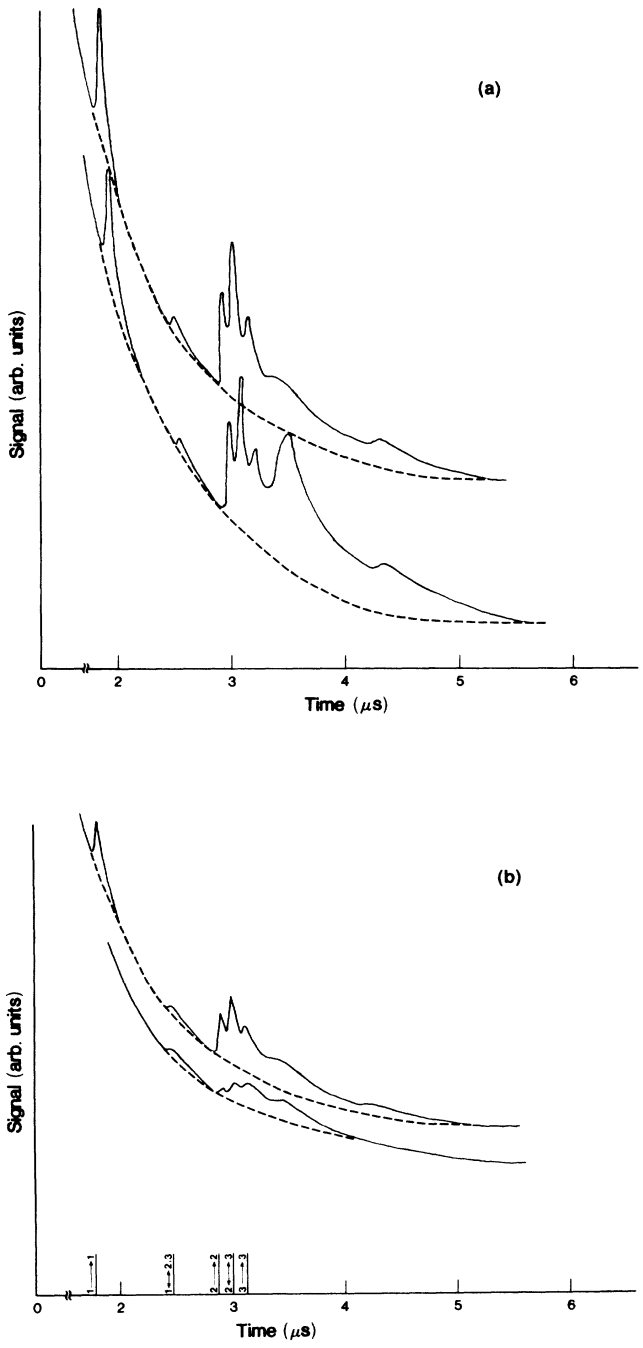

FIG. 12. (a) Reflection signal showing the effect of 7.5-keV Ar sputtering of the gold film (on sapphire) on the diffuse peak [see the inset of Fig. 7(a)]. The upper trace is the signal prior to irradiation and the lower curve is taken after all the gold is sputtered away. The dashed curves are spline fits to the background. (b) Phonon-reflection signal showing the effect of 7.5-keV Ar sputtering of the gold film (overlaid on sapphire) on the specular peaks [see the inset of Fig. 7(b)]. The upper curve is the signal from a virgin crystal (with 750 Å of Au) whereas in the lower trace, the ion beam has completely sputtered the gold film away. The dashed curves are spline fits to the background.

the height of the diffuse peak for the uncoated virgin surface. The difference between the values marked with the circle (○) and the cross (×) is to be attributed to the effect of the sputtering beam and is in fact comparable to the results of the 1 MeV implantation [Fig. 9(b)]. Thus, once the effect of the gold film removal is taken into account, the increase in the diffuse peak resembles that of the 1 MeV implantation.

It is worth pointing out that the decline in the specular peaks is saturated when only about 400 Å of the gold is removed, long before the damage reaches the surface of Al_2O_3. This is not surprising; due to an almost perfect acoustical match between Au and Al_2O_3 at near normal incidence, there is practically no reflection at the Au-Al_2O_3 interface and the specular peaks are caused by reflection at the surface of the gold film.

We then introduced thermal Ar atoms to the surface. While the specular peaks remained unaffected, the adsorbed film led to a dramatic suppression of the diffuse signal, confirming our idea that the effect in this case is a surface phenomenon.

We also carried out the x-ray rocking measurements on this sample. We did not see any difference between that and the virgin crystal. The damaged region is too thin to be detected by this technique.

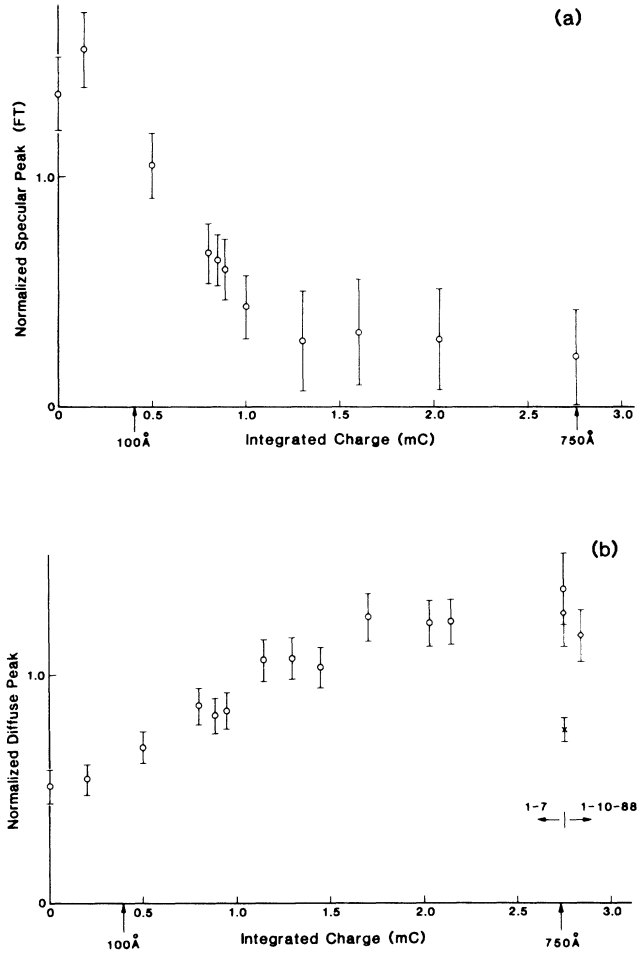

FIG. 13. (a) The height of the fast transverse peak, normalized to the unaffected amplitude of the diffuse peak, as a function of the amount of gold removed. Note that the signal is saturated by the time 300 Å of Au is removed in contrast to a more gradual enhancement of the diffuse peak (b). Also in this case, the specular peaks are almost completely gone in contrast to a factor of 2 reduction in the MeV implantation case. (b) The height of the diffuse peak, normalized to the unaffected amplitude of the fast transverse peak, as a function of the amount of the gold film removed. The circles (○) are the data taken on January 7, 1988 whereas the diamonds (◇) are the data taken on January 10, 1988. Between these two runs, the crystal was warmed up to room temperature and cooled back down. Again we see an indication of some possible annealing of the induced damage. The cross (×) indicates the height of the diffuse peak for a virgin crystal without the gold film (see the text).

IV. SUMMARY AND CONCLUSION

In summary, we have studied the effect of ion-beam-induced damage in sapphire single-crystals using scattering of thermal phonons (50-Å wavelength). In one case, a low-energy (7.5 keV) Ar^+ beam was used to sputter a thin film of Au overlaid on Al_2O_3 and in another series of experiments, a 1-MeV Ar^+ beam was implanted inside the crystal. In the former case, the damage was confined to within 80 Å of the surface, whereas in the MeV implantation, it extended 6500 Å into the material. Despite this difference, in both cases we observed a similar trend: a decline in the specular reflection signal along with a more gradual enhancement of the diffuse scattering. However, by adsorbing an Ar film onto the surface, we showed that in the low-energy case, the phonons were responding to the surface modification whereas in the MeV experiment, they were being scattered from the damage inside the material.

Pohl and Stritzker[15] have measured the low-temperature thermal conductivity of sapphire in the temperature range of 0.06 to 2.0 K, corresponding to phonon wavelengths of about 1.7 μm to 500 Å for transverse polarization. In this regime, the phonon mean free path is much longer than the size of the crystal and therefore the thermal conductivity will sensitively depend on whether the phonons are specularly or diffusely reflected at the surface of the sample. They observed that a 350-keV Xe^+ bombardment at a dose of 5×10^{15} ions/cm^2 as well as a 80-keV Xe^+ beam at a does of 5×10^{14} ions/cm^2 led to an increase in diffuse phonon scattering between 0.3 and 2 K. Even though they did not implant the ions *in situ* and only studied the effect at one dose, their observation is in general agreement with ours. However the wavelength of our phonons is about 50 Å ($\sim$19 K) and therefore we probed damage (on the surface or deeper inside) in a completely different length scale. On a more quantitative level, due to the higher frequencies of the phonons used in this investigation, we were able to resolve the surface modification (7.5-keV Ar^+ beam damage extended 80 Å inside the target) from the near surface damage (1-MeV Ar^+ beam damage peaked at 5500 Å). While in the former case our results quantitatively agree with those of Ref. 15, in the latter we see a reduction in the specular reflection that saturates at about $\frac{1}{2}$ of

that of the undamaged crystal (in contrast to its complete suppression as observed in our keV ion bombardment as well as the results reported by Pohl and Stritzker[15]).

Finally, in this paper we have investigated the feasibility of using THz ballistic phonons as a surface and near-surface probe. We have shown that with this technique we are able to probe modifications both on the surface (sputtering damage) and deeper inside the material (ion implantation). However, at present, we lack quantitative understanding of some of the results. The reason for this is twofold. On the one hand, one would like to have a more accurate description of the effect of the ion beams on the target. This concern showed up in the x-ray rocking measurements of the damage (i.e., the long decaying tail of the x-ray reflection signal). On the other hand, at present a theory of phonon propagation in a radiation-damaged lattice is not available, at least in the region where the mean separation between induced defects becomes comparable to the wavelength of the phonons.[28]

ACKNOWLEDGMENTS

We wish to acknowledge N. N. Asplund, A. P. Rice, F. Scaramuzzi, D. M. Strayer, T. Vreeland, Jr., D. L. Weathers, and F. Xiong for their valuable contributions to the course of this research. This work was supported by U.S. Department of Energy (DOE) Contract No. DE-FG03-85ER-45192. ne of us (T.A.T.) was supported in part by the National Science Foundation under Grant No. DMR 86-15641.

---

*Present address: Department of Chemistry, Pennsylvania State University, University Park, PA 16802.

†Present address: W. K. Kellogg Radiation Laboratory, California Institute of Technology, 106-38, Pasadena, CA 91125.

[1]P. Taborek and D. L. Goodstein, J. Phys. C **12**, 4737 (1979).

[2]P. Taborek and D. L. Goodstein, Phys. Rev. B **22**, 1550 (1980).

[3]For a review article on heat transmission between two solids see A. C. Anderson, in *Nonequilibrium Superconductivity, Phonons and Kapitza Boundaries,* edited by K. E. Gray (Plenum, New York 1980), p. 1.

[4]For a review article on heat transmission across a solid-LHe interface see A. F. G. Wyatt, Ref. 3, p. 31.

[5]D. L. Goodstein, R. Maboudian, F. Scaramuzzi, M. Sinvani, and G. Vidali, Phys. Rev. Lett. **55**, 2034 (1985).

[6]M. Sinvani, D. L. Goodstein, M. W. Cole, and P. Taborek, Phys. Rev. B **30**, 1231 (1984).

[7]For a review article see D. L. Goodstein, in *Nonequilibrium Phonon Dynamics, NATO Advanced Study Institute,* edited by W. E. Bron (Plenum, New York, 1985), p. 623.

[8]For a review article see R. J. Von Gutfeld, in *Physical Acoustics,* edited by W. P. Mason (Academic, New York, 1968), Vol. V, p. 233.

[9]V. B. Braginsky, V. P. Mitrofanov, and V. I. Panov, *Systems with Small Dissipation* (The University of Chicago Press, Chicago, 1985).

[10]J. Weber, W. Sandmann, W. Dietsche, and H. Kinder, Phys. Rev. Lett. **40**, 1469 (1978).

[11]H. C. Basso, W. Dietsche, H. Kinder, and P. Leideres, in *Phonon Scattering in Condensed-Matter,* edited by W. Eisenmenger *et al.* (Springer, New York, 1984), p. 212.

[12]P. Taborek and D. L. Goodstein, Solid State Commun. **38**, 215 (1981), and some other unpublished results.

[13]H. Kinder, Physica B+C, **107B**, 549 (1981).

[14]A. Khater and J. Szeftel, Phys. Rev. B **35**, 6749 (1987), and references therein.

[15]R. O. Pohl and B. Stritzker, Phys. Rev. B **25**, 3608 (1982).

[16]T. Klitsner and R. O. Pohl, in *Phonon Scattering in Condensed Matter,* edited by W. Eisenmenger *et al.* (Springer, New York, 1984), p. 188.

[17]T. Klitsner and R. O. Pohl, in *Phonon Scattering in Condensed Matter,* edited by A. C. Anderson and J. P. Wolfe (Springer, New York, 1986), p. 162.

[18]For a review article see T. Vreeland, Jr. and B. M. Paine, J. Vac. Sci. Technol. A **4**, 3153 (1986).

[19]J. F. Ziegler, J. P. Biersack, and U. Littmark, *The Stopping and Range of Ions in Solids* (Pergamon, New York, 1985), Vol. 1, Chap. 4.

[20]Originally, a premium-quality (Hemex) sapphire crystal grown by Crystal System Inc. (using the heat-exchanger method) was obtained with a chemi-mechanically polished surface. Much to our surprise, the whole reflection signal (specular as well as diffuse component) was noticeably smaller than in the previous investigation (Refs. 1 and 2) indicating a poorer quality bulk crystal as far as the propagation of THz phonons was concerned. This might be a consequence of higher concentration of F^+ centers in the crystals grown by the Crystal System Inc. as reported by J. D. Brewer, B. J. Jeffries, and G. P. Summers, Phys. Rev. B **22**, 4900 (1980).

[21]P. S. P. Wei and A. W. Smith, J. Vac. Sci. Technol. **9**, 1209 (1972).

[22]The gold film is easily peeled off by a piece of adhesive tape.

[23]R. E. Horstman and J. Wolter, Phys. Lett. **62A**, 279 (1977).

[24]Yuanxum Qui, J. E. Griffith, and T. A. Tombrello, Radiat. Effects **64**, 111 (1982).

[25]V. S. Speriosu, J. Appl. Phys. **51**, 6094 (1981).

[26]C. R. Wie, T. Vreeland, Jr., and T. A. Tombrello, Mater. Res. Soc. Symp. Proc. **35**, 305 (1985).

[27]CaF_2 is the only insulator which has been investigated by this technique for which the long tail we observed here is missing. See Ref. 26.

[28]For a treatment of this problem in the case of dilute static imperfections see P. G. Klemens, Proc. Phys. Soc. A **68**, 1113 (1955).